A Riemann Solver for Wet/Dry Interfaces in Finite Volume Schemes

Brian KYANJO   Prof. Donna Calhoun

Department of Mathematics
Boise State University

November 8, 2021

Outline

Introduction

A tsunami: is a series of energetic water waves generated due to the displacement of large volumes of water by different mechanisms such as earthquakes, volcanic eruptions, underwater landslides, and local landslides along the coast.

Recent tragic events:

- ▶ Tsunami of August 29, 2018 (Loyalty Islands)
- ▶ Tsunami of May 15, 2018 (Northeast Coast, US)
- ▶ Tsunami of January 23, 2018 (Off Kodiak Island, AK)
- ▶ Tsunami of July 17, 2017 (Western Aleutian Islands)
- ▶ Tsunami of May 1, 2017 (Elfin Cove)

Damages: Loss of human lives and devastating damages to infrastructures.

Tsunami impacts

Figure: Waves approach Miyako City after a 9.0 magnitude earthquake hit Japan. This tsunami led to more than 15,000 deaths. ▸ Link

Motivations

Deep knowledge of tsunamis is required to provide early warning messages to the regions that may be affected, carry out:

- ▶ Necessary evacuations
- ▶ Anticipate the highest run-ups and run-downs

Most numerical tsunami models rely on solving Riemann problems which can robustly track wetting and drying interfaces to model run-up on beaches and inundation into harbors and communities along the affected coastlines.

SWE for tsunami modeling

Shallow water models have been frequently used to handle the propagation of tsunami waves in the ocean see for instance Dutykh and Dias (2007); LeVeque et al. (2011); Dias and Dutykh (2007).

The Shallow water wave equations, given by

$$h_t + (hu)_x = 0$$
$$(hu)_t + \left(hu^2 + \frac{1}{2}\rho g h^2\right)_x = 0 \tag{1}$$

is an example of a system of equations written in conservative form.

1D Riemann problem

At each cell interface, solve the hyperbolic problem with initial data, i.e.

$$q_t + f(q)_x = 0 \tag{2}$$

subject to

$$q(x,0) = \begin{cases} q_l, & \text{if } x \leq 0, \\ q_r, & \text{if } x > 0, \end{cases} \tag{3}$$

At $x = 0$ and $t = 0$, the discontinuity is located between the left and right state, so the solution at the left (q_l) and right(q_r) states are given by:

$$q_l = \begin{bmatrix} h_l \\ (hu)_l \end{bmatrix} \quad \text{and} \quad q_r = \begin{bmatrix} h_r \\ (hu)_r \end{bmatrix} \tag{4}$$

1D Riemann Solution

As t increases, four distinct regions are created, separated by
characteristics. The middle state (q_m) is generated.
The determination of this state characterizes the Riemann
problem and how it connects to other states via waves in each
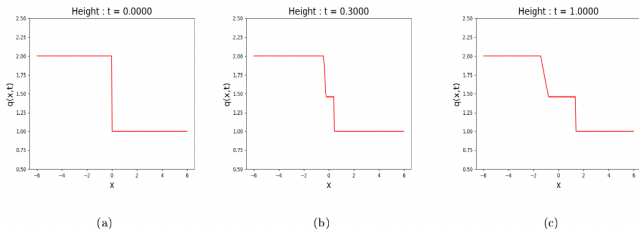respective characteristic family.
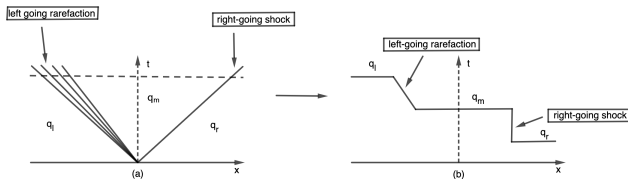
Figure: x-t plane showing the connection of states, *left-going
rarefaction*, and the *right-going shock*.

Evolution of the Riemann solution

This solutions are produced by the exact Riemann solver after applying $h_l = 2$, $h_r = 1$, and $u_l = u_r = 0$ as initial conditions in the Riemann problem.

(a)   (b)   (c)

Figure: Temporal evolution of the height field solution for the dam break problem with *left-going rarefaction* and a *right-going shock*. See Artifact for code that produced these plots.

Approximate methods are widely used due to their cheap computational cost compared to the exact solvers (Roe (1981)).

Exact Riemann solver for two-shock SWE

General left, and right states will be connected by a combination
of the two (either two shocks, two rarefactions, or one of each).
**Ways to achieve an exact Riemann solution:**
The shock speed, $s(t)$, from the shock wave as the solution
emerges is determined from the Rankine-Hugoniot jump
condition which must be satisfied across any shock wave.

$$s_1(q_m - q_l) = f(q_m) - f(q_l)$$
$$s_2(q_r - q_m) = f(q_r) - f(q_m)$$

(5)

The Rankine Hugoniot conditions will be satisfied, if q_l and q_r
are connected by a shock, (LeVeque et al. (2002); Toro (2001)).

Hugoniot loci

By applying Rankine-Hugoniot jump condition to shallow water equations creates a system of four equations that must be satisfied simultaneously.
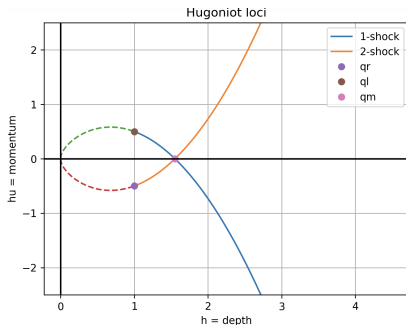
Figure: Shows curves that represent all states connected to q_l and all states connected to q_r via a *2-shock* and *1-shock* respectively. See Artifact for code that produced these plots.

Exact Riemann solution

This solutions are produced by the exact Riemann solver after applying $h_l = h_r = 1$, $u_l = 0.5$, and $u_r = -0.5$ as initial conditions in the Riemann problem.
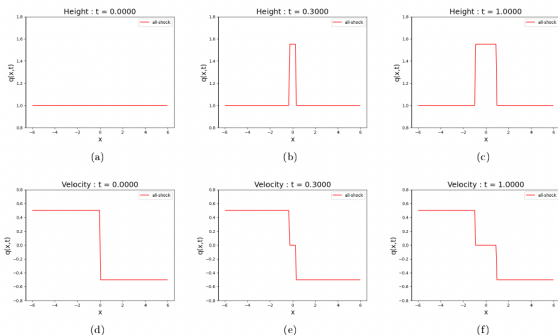
Figure: Temporal evolution of the height and velocity field solution for the all-shock case with *left-going shock* and a *right-going shock*. See Artifact for code that produced these plots.

General Case

The Lax entropy condition requiring that $h_m > h_l, h_r$ may not be satisfied in all cases. We can also connect states by a rarefaction wave.

(a)　　　　　　　　(b)　　　　　　　　(c)
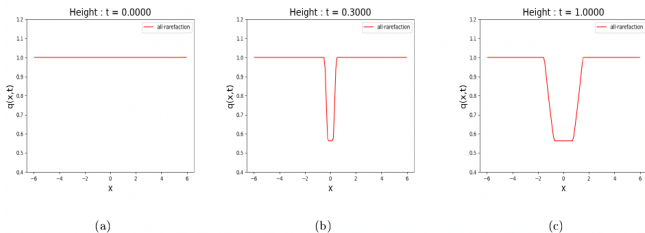
Figure: Temporal evolution of the height field solution for the all-rarefaction case with *left-going rarefaction* and a *right-going rarefaction*. See Artifact for code that produced these plots.

Finite volume discretization

Finite volume discretizations are widely used in tsunami modeling since they are:

▶ Well suited for inundation regimes

▶ Robust in the presence of drying regions

▶ Well-balanced

▶ Can capture the inundating shoreline and run-up features

George (2008, 2011, 2006); Berger et al. (2011); Bi et al. (2014); LeVeque et al. (2002); Bale et al. (2003).

Finite volume discretization

Assume a conservation law of the form

$$q_t + f(q)_x = 0 \tag{6}$$

Define cell averages over the interval $C_i = (x_{i-\frac{1}{2}}, x_{i+\frac{1}{2}})$

$$Q_i^n \approx \frac{1}{\Delta x} \int_{C_i} q(x, t^n) dx \tag{7}$$

How does the average evolve?

$$
\begin{aligned}
\frac{d}{dt} \int_{c_i} q(x,t) dx &= -\int_{c_i} \frac{d}{dx} f(q(x,t)) dx \\
&= f(q(x_{i-\frac{1}{2}}, t)) - f(q(x_{i+\frac{1}{2}}, t))
\end{aligned} \tag{8}
$$

Finite volume discretization

Integrate in time

$$
\begin{aligned}
\int_{c_i} q(x, t_{n+1})dx = \int_{c_i} q(x, t_n)dx \\
+ \int_{t_n}^{t_{n+1}} [f(q(x_{i-\frac{1}{2}}, t_n)) - f(q(x_{i+\frac{1}{2}}, t_n))]dt
\end{aligned}
\tag{9}
$$

This leads to the update formula:

$$
Q_i^{n+1} = Q_i^n - \frac{\Delta t}{\Delta x}(F_{i+\frac{1}{2}}^n - F_{i-\frac{1}{2}}^n)
\tag{10}
$$

Reducing to the original Godunov first order accurate scheme Godunov (1959).

$$
Q_i^{n+1} = Q_i^n - \frac{\Delta t}{\Delta x}[\mathcal{F}(Q_i, Q_{i+1}) - \mathcal{F}(Q_{i-1}, Q_i)]
\tag{11}
$$

Finite volume discretization

Different finite volume schemes will include higher order time stepping and or spatial terms to increase accuracy.
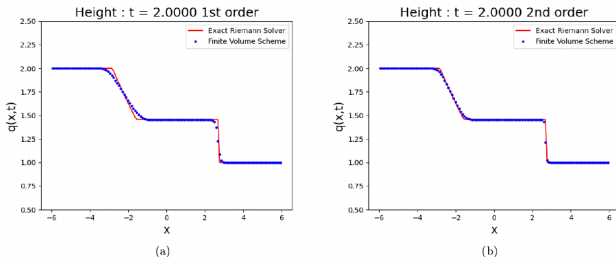
Figure: (a) and (b) respectively show height field at the final time step for both first and second order correction with limiters for the exact and approximate solutions. See Artifact for code that produced these plots.

Finite schemes in quasi-linear form

Another approach to solving conservation laws is to write them in *quasilinear form* and develop numerical methods based on an eigen-decomposition of the Jacobian matrix.

$$q_t + f'(q)q_x = 0 \tag{12}$$

Subject to Riemann problem with initial data

$$q(x, t^n) = \begin{cases} Q_{i-1}^n & \text{if} \quad x < x_{i-\frac{1}{2}} \\ Q_i^n & \text{if} \quad x > x_{i-\frac{1}{2}} \end{cases} \tag{13}$$

Wave Propagation algorithm (WPA)

Here the formalism of the WPA, first described in LeVeque (1997) is presented.

The initial data, is used by the exact Riemann solver to generate an intermediate state ($q_m = (h_m, hu_m)^T$), which is used to evaluate the eigenvalues ($\lambda_{i-1/2}$) and eigenvectors ($r_{i-1/2}$) at $x = x_{i-\frac{1}{2}}$.

The pth wave at the $i - \frac{1}{2}$ interface is given by

$$\mathcal{W}^p_{i-1/2} \equiv \alpha_{i-\frac{1}{2}} r^p_{i-\frac{1}{2}}$$

with speeds

$$s^p_{i-1/2} = \lambda^p_{i-1/2}$$

WPA

Waves and speeds are obtained as an eigenvector decomposition of the jump in Q_i at the interface $i - \frac{1}{2}$. This decomposition takes the form

$$Q_i - Q_{i-1} = \sum_{p=1}^{m} \alpha_{i-\frac{1}{2}} r_{i-\frac{1}{2}} \equiv \sum_{p=1}^{m} \mathcal{W}_{i-\frac{1}{2}}^{p} \tag{14}$$

The fluctuations $\mathcal{A}^{+} \Delta Q_{i-\frac{1}{2}}^{n}$ and $\mathcal{A}^{-} \Delta Q_{i-\frac{1}{2}}^{n}$ are given by

$$\mathcal{A}^{-} \Delta Q_{i-\frac{1}{2}}^{n} = \sum_{\{p : s_{i-\frac{1}{2}}^{p} < 0\}} s_{i-\frac{1}{2}}^{p} \mathcal{W}_{i-\frac{1}{2}}^{p} \tag{15}$$

$$\mathcal{A}^{+} \Delta Q_{i-\frac{1}{2}}^{n} = \sum_{\{p : s_{i-\frac{1}{2}}^{p} > 0\}} s_{i-\frac{1}{2}}^{p} \mathcal{W}_{i-\frac{1}{2}}^{p} \tag{16}$$

MUSCL approach

Monotone upstream-centered scheme for conservation laws (MUSCL) is a FVM that was developed by Van Leer (1979) to build the first high-order and high-resolution total variation diminishing techniques for hyperbolic PDEs.

Many researchers such as (Song et al. (2011); Zhao et al. (2019); Marche et al. (2007); Liang and Borthwick (2009)), have widely used MUSCL schemes to solve two-dimensional SWEs due to their:

- ▶ Monotonicity
- ▶ Stability preservation
- ▶ More significant order of accuracy by data reconstruction

These methods are extensions of the original Godunov scheme.

Bathymetry

The second challenge in modeling tsunamis is in proper treatment of the bathymetry, or variable ocean bottom.

$$h_t + (uh)_x = 0$$
$$(hu)_t + \left(hu^2 + \frac{1}{2}gh^2 \right)_x = - ghB'(x). \tag{17}$$

General source terms are typically handled in an operator split approach.

However, for tsunami modeling, this can lead to oscillations in steady state solutions. An approach described by Bale et al. (2003) and based on the WPA is to discretise the source term to generate values $-gh_{i-\frac{1}{2}}B'(x_{i-\frac{1}{2}})$ at cell interfaces $x = x_{i-\frac{1}{2}}$.

Bathymetry

This approach is very useful, because the discrepancy caused due to the failure of the flux gradient to counterbalance the source term in a near steady state solution is decomposed into propagating waves making the approach more robust than the quasi-steady wave propagation algorithm .
This makes the scheme

- ▶ Well balanced
- ▶ Preserve depth positivity
- ▶ Able to model shifts between wet/dry regions

Beach run-up and inundation

The wetting and drying processes have significant physical and biological impacts on shallow water systems and coastal environments.

They can arise due to inundation effects on coastal mudflats and wave-driven run-up on beaches and dunes on periodic time scales, i.e.,

- ▶ Several hours for the rise and fall of the tide
- ▶ Several days for storm surge
- ▶ Infragravity wave motions on the shoreface

These effects can cause extreme devastating damages and coastal erosion.

Riemann Problem for Wet/Dry states

Dry states are regions with zero water depth. In such states
SWEs are not applicable, so we consider wet states adjacent to
dry regions. This enables solving SWEs in wet states, right up
the boundary between wet and dry states Toro (2001); George
(2008).
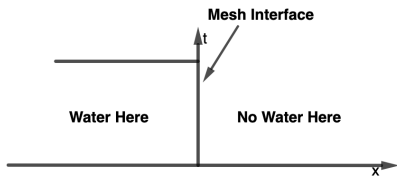
Figure: The Riemann problem with a dry bed (has no water) in one of
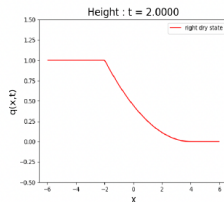the data state.

The solution was obtained using Toro's method implemented in the exact Riemann solver with intial coditions: $h_l = 1$, $h_r = 0$, and $u_l = u_r = 0$ described below.

(a)   (b)   (c)
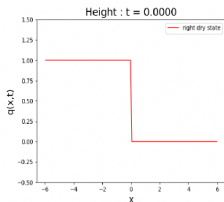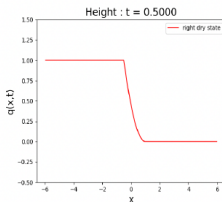
Figure: Temporal evolution of the height field solution for the right dry state case. See Artifact for code that produced these plots.

Various Approaches to handling wet/dry interfaces

We describe different methods that appear in the literature for handling the wetting and drying problems.

- ▶ **Four elevation modification method:** Liu et al. (2021) also used the Godunov-type finite volume methods to process dry and wet/dry front cells to predict flood elevation by taking four elevation modifications.

- ▶ **Relaxation method:** Pelanti et al. (2011) formulated a Riemann solver based on the relaxation approach for both single-phase and double-phase shallow flow equations explaining a mixture of granular material and fluid.

- ▶ **Contact discontinuity Method:** Toro (2001) solved a Riemann problem with cases in which the dry regions are either present at the initial time or appear as a result of the interaction of two wet bed states.

Various Approaches to handling wet/dry interfaces

- **Galerkin approach:** Bunya et al. (2009), proposed that the wetting and drying can also be handled by the linear piecewise Runge-Kutta discontinuous Galerkin approximation (RKDG) to SWE solutions.
- **Adaptive approach:** Popinet (2011) modeled the 2004 Indian ocean tsunami using adaptive modeling by generalizing the Audusse et al. (2004) well-balanced and positivity preserving scheme for solving the Saint-Venant equations with wetting and drying to an adaptive quadtree spatial discretization.
- Augmented Riemann solver (George)

Augmented Riemann solver (George)

In George (2008, 2011), a method for handling wetting and drying in the wave propagation algorithm is described. Consider wave and speed decomposition given by

$$Q_i - Q_{i-1} = \sum_{p=1}^{m} \alpha_{i-\frac{1}{2}} r_{i-\frac{1}{2}} \equiv \sum_{p=1}^{m} \mathcal{W}_{i-\frac{1}{2}}^p \qquad (18)$$

Replace with

$$\begin{bmatrix} H_i - H_{i-1} \\ HU_i - HU_{i-1} \\ \varphi(Q_i) - \varphi(Q_{i-1}) \end{bmatrix} = \sum_{p=1}^{3} \alpha_{i-\frac{1}{2}}^p w_{i-\frac{1}{2}}^p \qquad (19)$$

Augmented Riemann solver (George)

The decomposition of the solutions $Q_i - Q_{i-1}$ and $f(Q_i) - f(Q_{i-1}) \in \mathbb{R}^2$ are represented by the first two and last two components of the three components of the decomposition. Then consider $z^p_{i-\frac{1}{2}} \in \mathbb{R}^2$ for each $p \in [1,3]$ to be flux waves defined by:

$$z^p_{i-\frac{1}{2}} = [\mathbf{0}_{2\times1} \quad \mathbf{I}_{2\times2}] \alpha^p_{i-\frac{1}{2}} w^p_{i-\frac{1}{2}} \tag{20}$$

Then updated fluctuations become:

$$\mathcal{A}^+ \Delta Q^n_{i-\frac{1}{2}} = \sum_{\{p:s^p_{i-\frac{1}{2}}>0\}} z^p_{i-\frac{1}{2}} \tag{21}$$

$$\mathcal{A}^- \Delta Q^n_{i+\frac{1}{2}} = \sum_{\{p:s^p_{i+\frac{1}{2}}<0\}} z^p_{i+\frac{1}{2}} \tag{22}$$

Augmented Riemann solver (George)

The decomposition of the four variables: depth, momentum, momentum flux, and bathymetry into four propagating waves give the solver unique features:

- ▶ Riemann problems with a large rarefaction are accurately more approximated
- ▶ A natural entropy fix for transonic rarefactions
- ▶ Stationery oceans at a steady-state and discretized smooth
- ▶ Steady states over variable bathymetry are preserved
- ▶ Shockwave solution is captured due to the solver's equivalency to the Roe solver

In the absence of the source term, the solver preserves depth negativity and is well balanced in the presence of a source term.

Future research directions

- Numerics
  - Cases when eigenvalues of the Jacobian matrix change sign. Results show that the available approaches (Bale et al. (2003))
  - Higher order, different grids; We are also interested in implementing SWE on a cubed sphere grid with adaptive mesh refinement (AMR) (McCorquodale et al. (2015)).
  - More robust treatment of wet-dry states is still needed since existing methods are not perfect.
- Modeling
  - Tsunamis detection in real-time through observation of signals in the atmosphere (Meng et al. (2015); Hickey et al. (2009))
  - Coupling to other codes; existing software for predicting tsunamis can be incorporated with other atmospheric models to improve forecasts.
  - Dispersive corrections in SWE model (Lannes and Bonneton (2009); Popinet (2020, 2015)).

Future Research Directions

- Hardware/software
  - Parallel implementation of SWE models (Qin et al. (2018))
  - Testing SWE on software with adaptivity: forestclaw (Berger et al. (2011)) and Basilisk (Popinet (2015))

Artifact

This artifact we implemented the three approximate solvers for solving Riemann problem and an exact solver for handling wet/dry interfaces.

- ▶ The Artifact is completely done in python.
- ▶ It consists of three python scripts:
  - ▶ approximate_solver.py
  - ▶ exact_solver.py
  - ▶ test.py
- ▶ It consists of a main notebook: **main.ipynb** in which simulations are performed.
- ▶ The README file explains the usage
- ▶ Contains a mathematical documentation
- ▶ It is also available on GitHub: ▶ Link

Thank you!

briankyanjo@u.boisestate.edu

References I

Audusse, E., Bouchut, F., Bristeau, M.-O., Klein, R., and Perthame, B. t. (2004). A fast and stable well-balanced scheme with hydrostatic reconstruction for shallow water flows. *SIAM Journal on Scientific Computing*, 25(6):2050–2065.

Bale, D., LeVeque, R. J., Mitran, S., and Rossmanith, J. (2003). A Wave Propagation Method for Conservation Laws and Balance Laws with Spatially Varying Flux Functions. 24(3):955–978.

Berger, M. J., George, D. L., LeVeque, R. J., and Mandli, K. T. (2011). The GeoClaw software for depth-averaged flows with adaptive refinement. 34(9):1195–1206. arXiv:1008.0455v2 [physics.geo-ph].

Bi, S., Zhou, J., Liu, Y., and Song, L. (2014). A finite volume method for modeling shallow flows with wet-dry fronts on adaptive cartesian grids. *Mathematical problems in Engineering*, 2014.

Bunya, S., Kubatko, E. J., Westerink, J. J., and Dawson, C. (2009). A wetting and drying treatment for the Runge–Kutta discontinuous Galerkin solution to the shallow water equations. *Comput. Method Appl. M.*, 198(17):1548–1562.

References II

Dias, F. and Dutykh, D. (2007). Dynamics of tsunami waves. In *Extreme man-made and natural hazards in dynamics of structures*, pages 201–224. Springer.

Dutykh, D. and Dias, F. (2007). Water waves generated by a moving bottom. In *Tsunami and Nonlinear waves*, pages 65–95. Springer.

George, D. L. (2006). Finite volume methods and adaptive refinement for tsunami propagation and inundation.

George, D. L. (2008). Augmented Riemann solvers for the shallow water equations over variable topography with steady states and inundation. *J Comp Phys*, 227(6):3089 – 3113.

George, D. L. (2011). Adaptive finite volume methods with well-balanced Riemann solvers for modeling floods in rugged terrain: Application to the Malpasset dam-break flood (France, 1959). 66(8):1000–1018.

Godunov, S. K. (1959). A difference scheme for numerical solution of discontinuous solution of hydrodynamic equations. *Math. Sbornik*, 47:271–306.

References III

Hickey, M. P., Schubert, G., and Walterscheid, R. (2009). Propagation of tsunami-driven gravity waves into the thermosphere and ionosphere. *Journal of Geophysical Research: Space Physics*, 114(A8).

Kubatko, E. J., Westerink, J. J., and Dawson, C. (2007). Semi discrete discontinuous galerkin methods and stage-exceeding-order, strong-stability-preserving runge–kutta time discretizations. *Journal of Computational Physics*, 222(2):832–848.

Lannes, D. and Bonneton, P. (2009). Derivation of asymptotic two-dimensional time-dependent equations for surface water wave propagation. *J. Comput. Phys.*, 21:016601–1–9.

LeVeque, R. J. (1997). Wave Propagation Algorithms for Multidimensional Hyperbolic Systems. *J. Comput. Phys.*, 131(2):327–353.

LeVeque, R. J. et al. (2002). *Finite volume methods for hyperbolic problems*, volume 31. Cambridge university press.

References IV

LeVeque, R. J., George, D. L., and Berger, M. J. (2011). Tsunami modelling with adaptively refined finite volume methods. 20:211 – 289.

Liang, Q. and Borthwick, A. G. (2009). Adaptive quadtree simulation of shallow flows with wet–dry fronts over complex topography. *Computers & Fluids*, 38(2):221–234.

Liu, D., Tang, J., Wang, H., Cao, Y., Bazai, N. A., Chen, H., and Liu, D. (2021). A New Method for Wet-Dry Front Treatment in Outburst Flood Simulation. *Water*, 13(2).

Marche, F., Bonneton, P., Fabrie, P., and Seguin, N. (2007). Evaluation of well-balanced bore-capturing schemes for 2d wetting and drying processes. *International Journal for Numerical Methods in Fluids*, 53(5):867–894.

McCorquodale, P., Ullrich, P., Johansen, H., and Colella, P. (2015). An adaptive multiblock high-order finite-volume method for solving the shallow-water equations on the sphere. *Communications in Applied Mathematics and Computational Science*, 10(2):121–162.

References V

Meng, X., Komjathy, A., Verkhoglyadova, O., Yang, Y.-M., Deng, Y., and Mannucci, A. (2015). A new physics-based modeling approach for tsunami-ionosphere coupling. *Geophysical Research Letters*, 42(12):4736–4744.

Pelanti, M. and Bouchut, F. (2008). A relaxation method for modeling two-phase shallow granular flows. In *Proceedings of Symposia in Applied Mathematics*, volume 67, pages 835–844.

Pelanti, M., Bouchut, F., and Mangeney, A. (2011). A riemann solver for single-phase and two-phase shallow flow models based on relaxation. relations with roe and vfroe solvers. *Journal of Computational Physics*, 230(3):515–550.

Popinet, S. (2011). Quadtree-adaptive tsunami modelling. *Ocean Dynamics*, 61(9):1261–1285.

Popinet, S. (2015). A quadtree-adaptive multigrid solver for the Serre–Green–Naghdi equations. *J. Comput. Phys.*, 302:336 – 358.

Popinet, S. (2020). A vertically-Lagrangian, non-hydrostatic, multilayer model for multiscale free-surface flows. *J. Comput. Phys.*, 418:109609.

References VI

Qin, X., LeVeque, R. J., and Motley, M. (2018). Accelerating wave-propagation algorithms on adaptive mesh with the graphics processing unit (GPU). *(submitted)*.

Roe, P. L. (1981). Approximate riemann solvers, parameter vectors, and difference schemes. *Journal of computational physics*, 43(2):357–372.

Song, L., Zhou, J., Guo, J., Zou, Q., and Liu, Y. (2011). A robust well-balanced finite volume model for shallow water flows with wetting and drying over irregular terrain. *Advances in Water Resources*, 34(7):915–932.

Toro, E. F. (2001). *Shock-capturing methods for free-surface shallow flows*. Wiley-Blackwell.

Van Leer, B. (1979). Towards the ultimate conservative difference scheme. v. a second-order sequel to godunov's method. *Journal of computational Physics*, 32(1):101–136.

Zhao, J., Özgen-Xian, I., Liang, D., Wang, T., and Hinkelmann, R. (2019). An improved multislope muscl scheme for solving shallow water equations on unstructured grids. *Computers & Mathematics with Applications*, 77(2):576–596.

Four elevation modification method (Liu et al.)

Liu et al. (2021) also used the Godunov-type finite volume methods to process dry and wet/dry front cells to predict flood elevation. This was done by taking four elevation modifications:

- ▶ Identifying four types of intercell through estimating their properties based on the depth of the flow and surface elevation difference
- ▶ Updating interface elevation depends on their properties to achieve gravity balance and prevent non-physical flux predictions
- ▶ Calculating dry cell's center elevations by taking the average of the two surrounding intercell elevations
- ▶ Modifying the first term of the slope limiter based on the elevation difference between intercell elevations dividing two times the mesh size

Relaxation method (Pelanti et al.)

Pelanti et al. (2011) formulated a Riemann solver based on the relaxation approach for both single-phase and double-phase shallow flow equations explaining a mixture of granular material and fluid.

- ▶ This approach is implemented by employing auxiliary variables to replace momenta in the spatial gradients of the original system.
- ▶ The eigenvalues of the relaxation model are determined from the coefficients of the linear equations governing the new auxiliary variables.
- ▶ The Riemann solution for the height of the flow and relaxation variables are calculated as Roe's Riemann solution.

This new solver is more robust in handling wet/dry interfaces (Pelanti and Bouchut (2008); Pelanti et al. (2011)).

Contact discontinuity Method (Toro)

According to Toro (2001), there are three possible cases to consider:

- ▶ Right dry bed, the solution exhibits a left-going rarefaction wave associated with the left eigenvalue $\lambda_1 = u - a$.
- ▶ Left dry bed, the solution exhibits right-going rarefaction wave associated with the right eigenvalue $\lambda_2 = u + a$.
- ▶ Dry bed doesn't exit at $t = 0$, but is created in the interaction between the two left and right wet bed regions if $S_{*L} \leq S_{*R}$ where $a = \sqrt{gh}$.
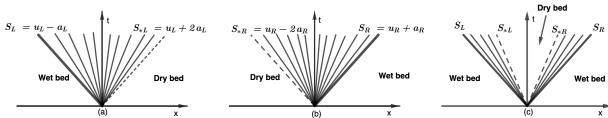
Galerkin approach (Bunya et al.)

The wetting and drying can also be handled by the linear piecewise Runge-Kutta discontinuous Galerkin approximation (RKDG) to SWE solutions. According to Bunya et al. (2009),

- ▶ This method is based on the thin water layer approach to optimize both computational cost and accuracy on fixed meshes.
- ▶ The water depth of each dry or partially wet element is tracked and controlled by updating water surface elevations at every end of each Runge-Kutta time step.
- ▶ This maintains the depth positivity of the water column yielding a stable solution over the entire domain for the SWE.

The technique's special treatment of numerical fluxes enables the water mass positivity in each element Bunya et al. (2009); Kubatko et al. (2007).

Adaptive approach (Popinet)

Popinet (2011) modeled the 2004 Indian ocean tsunami using adaptive modeling by:

▶ Generalizing the Audusse et al. (2004) well-balanced and positivity preserving scheme for solving the Saint-Venant equations with wetting and drying to an adaptive quadtree spatial discretization.

▶ Combining the wet/dry state solver with a Boussinesq solver to preserve the robustness of Saint-Venant solver.

The adaptive mesh refinement provided higher orders of magnitude gains in memory and speed when the approach was subjected to the dispersive wave propagations that occurred during the Tohoku tsunami.